MANCHESTER 1824

The University of Manchester

Superleading logarithms & subleading colour

Jeff Forshaw

With thanks to Andrea Banfi, Matthew De Angelis, Jack Holguin, Albrecht Kyrieleis, Simon Plätzer, Fernando Torre González, Mike Seymour

Outline

1. Back to the early 90s and rapidity gaps: Bjorken; Dokshizter, Khoze & Sjöstrand
2. Don’t work with empty gaps: Oderda & Sterman
3. Leftfield – non-global logs: Dasgupta & Salam
4. Attempting to understand NGLs gives SLLs
5. Super-super-leading logs
6. Beyond leading colour – results from `CVolver`

Rapidity gaps in Higgs production

Yu.L. Dokshitzer [1]
Department of Theoretical Physics, University of Lund, Sölvegatan 14A, S-223 62 Lund, Sweden

V.A. Khoze [1]
Centre for Particle Theory, University of Durham, Durham DH1 3LE, UK
and INFN Eloisatron project

and

T. Sjöstrand
CERN, CH-1211 Geneva 23, Switzerland

Received 11 October 1991

The possibility to discriminate different Higgs production mechanisms using a rapidity gap signature is discussed. The results of Monte Carlo calculations are presented, which show that the two processes WW→H and gg→H indeed have different event structures, but also that these differences, without special care, would be masked by other effects.

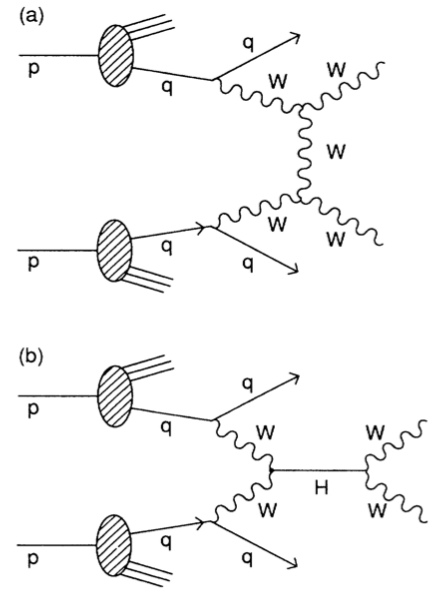

FIG. 1. Basic mechanism for producing W-W interaction processes in high-energy pp collisions, with the presence of a rapidity gap in the final state.

Rapidity gaps and jets as a new-physics signature in very-high-energy hadron-hadron collisions

J. D. Bjorken
Stanford Linear Accelerator Center, Stanford University, Stanford, California 94309
(Received 30 March 1992)

In hadron-hadron collisions, production of Higgs bosons and other color-singlet systems can occur via fusion of electroweak bosons, occasionally leaving a "rapidity gap" in the underlying-event structure. This observation, due to Dokshitzer, Khoze, and Troyan, is studied to see whether it serves as a signature for detection of the Higgs bosons, etc. We find it is a very strong signature at subprocess c.m. energies in excess of a few TeV. The most serious problem with this strategy is the estimation of the fraction of events containing the rapidity gap; most of the time the gap is filled by soft interactions of spectator degrees of freedom. We also study this question and estimate this "survival probability of the rapidity gap" to be of order 5%, with an uncertainty of a factor 3. Ways of testing this estimate and further discussion of the underlying hard-diffraction physics are presented.

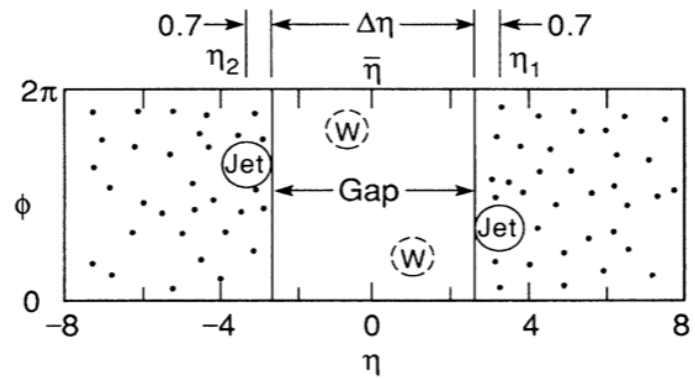

FIG. 2. Event morphology in lego variables for the processes depicted in Fig. 1. The tagging jets are the hadronization products of the quarks, while for large Higgs masses, almost all of the W-decay products lie within the dashed circles. The remaining region, marked gap, contains on average no more than 2 or 3 hadrons.

Two big challenges

1. “Gap survival” (Bjorken estimated 5% for SSC)

2. “Pomeron exchange” (Mueller-Tang 1992 & Del Duca-Tang 1993)

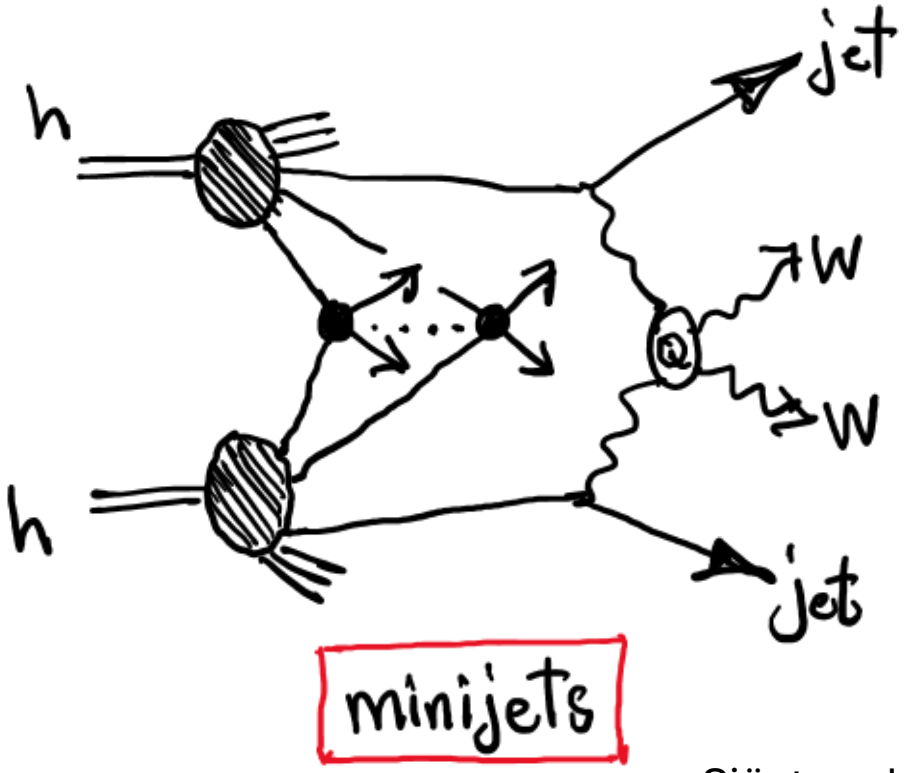

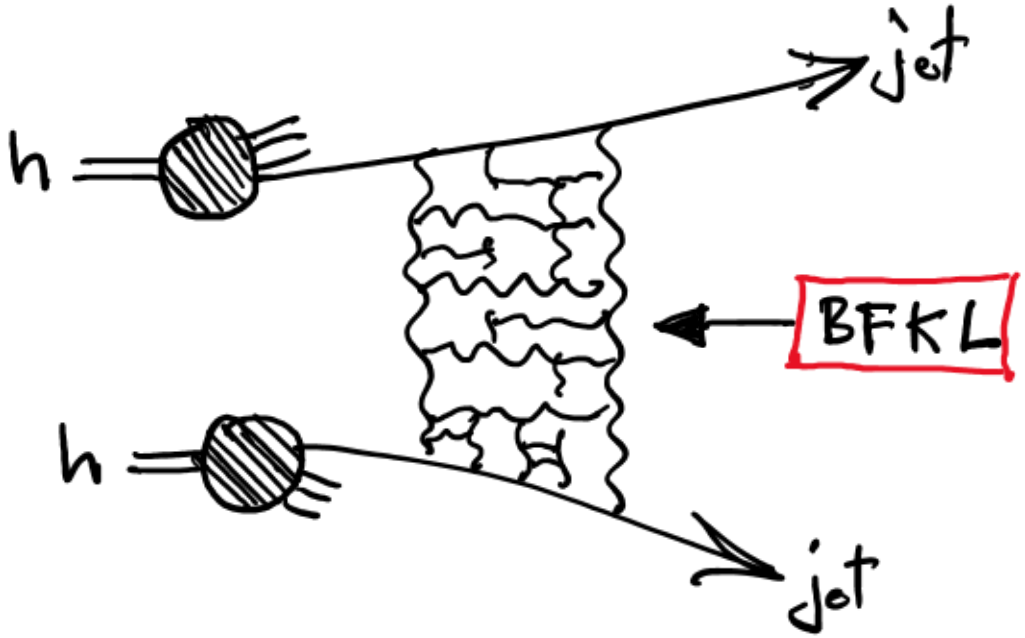

Sjöstrand & van Zijl 1987: underlying event

HERA and the Tevatron

Physics Letters B 315 (1993) 481–493
North-Holland

Observation of events with a large rapidity gap in deep inelastic scattering at HERA

ZEUS Collaboration

In deep inelastic, neutral current scattering of electrons and protons at $\sqrt{s} = 296$ GeV, we observe in the ZEUS detector events with a large rapidity gap in the hadronic final state. They occur in the region of small Bjorken x and are observed up to Q^2 of 100 GeV^2. They account for about 5% of the events with $Q^2 \geqslant 10$ GeV^2. Their general properties are inconsistent with the dominant mechanism of deep inelastic scattering, where color is transferred between the scattered quark and the proton remnant, and suggest that the underlying production mechanism is the diffractive dissociation of the virtual photon.

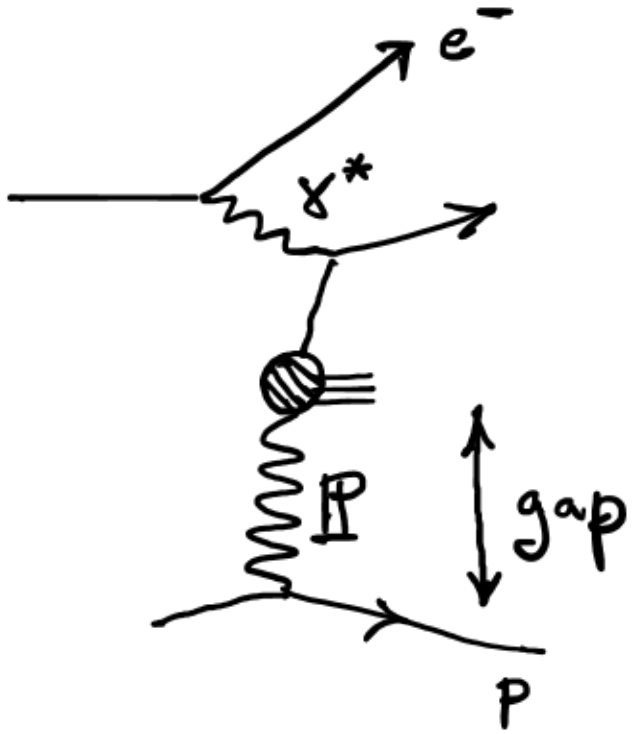

"*Proof of Factorization for Diffractive Hard Scattering*" (Collins 1997)
confirms the earlier conjecture of Kunszt-Stirling and Berera-Soper and generalizes the model of Ingelman-Schlein (1984) that predicted hard diffraction (UA8 1988)

But "gap survival" is process dependent

Recent work of Lee, Schindler & Stewart

Don’t work with empty gaps

Energy and Color Flow in Dijet Rapidity Gaps

Gianluca Oderda and George Sterman
Institute for Theoretical Physics, State University of New York at Stony Brook, Stony Brook, New York 11794-3840
(Received 30 June 1998)

Among the most intriguing recent experimental results in quantum chromodynamics is the observation of dijet rapidity-gap events, with anomalously low radiation in a wide interjet rapidity region [1–3]. These events are typically identified by low or zero hadron multiplicity in the central region, despite the high momentum transfer necessary to produce the jets.

The existence of such events was originally suggested on the basis of color flow considerations in QCD [4,5]. If forward jets are produced by exchanging a pair of gluons in a color singlet state, color can be recombined independently in each forward region. Then much less radiation is expected between the jets than when the exchange is a color octet gluon, which requires recombining color between particles moving in nearly opposite directions. Rapidity gap events have special interest as clear illustrations of color coherence and its interplay with hadronization. In addition, because their observation requires large rapidity intervals, they offer a new window into a perturbative, yet Regge-like limit of QCD. Nonetheless, despite their intuitive appeal, the theoretical understanding of rapidity gaps has been somewhat hampered by two problems. One of these is the issue of “survival” [5,6]. In any high-energy scattering, multiple soft interactions between spectators of the hard interaction may fill the gap by processes unrelated to the color content of the hard interaction. The second is that, since even the softest gluon carries color in the octet representation, it is not immediately obvious how the color of the hard scattering is to be defined.

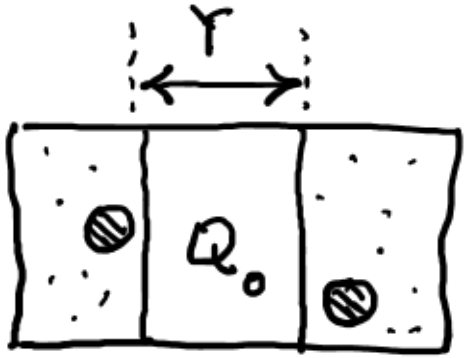

$$\frac{\mathrm{d}\sigma_{\mathrm{OS}}}{\mathrm{d}x_a \mathrm{d}x_b \,\mathrm{d}\mathcal{B}} = f_A(x_a, Q) f_B(x_b, Q) \mathrm{Tr}(\mathbf{V}_{Q_0,Q} \mathbf{H} \mathbf{V}^{\dagger}_{Q_0,Q}),$$

$$\mathbf{V}_{Q_0,Q} \approx \exp\left(-\frac{\alpha_s}{\pi} \ln \frac{Q}{Q_0} (Y \mathbf{T}_t^2 + i\pi \mathbf{T}_s^2)\right)$$

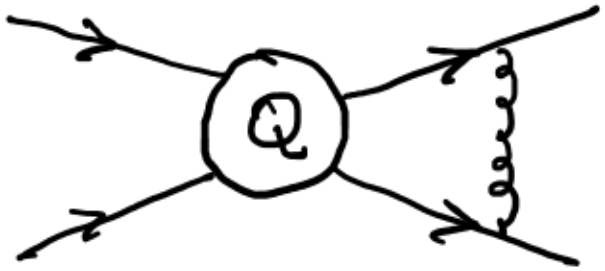

$Q \gg Q_0$ and Y large
subleading colour dominant

Wide-angle, soft gluons =
interplay of colour and kinematics

A fly in the ointment: the discovery of non-global logarithms

Dasgupta & Salam 2001

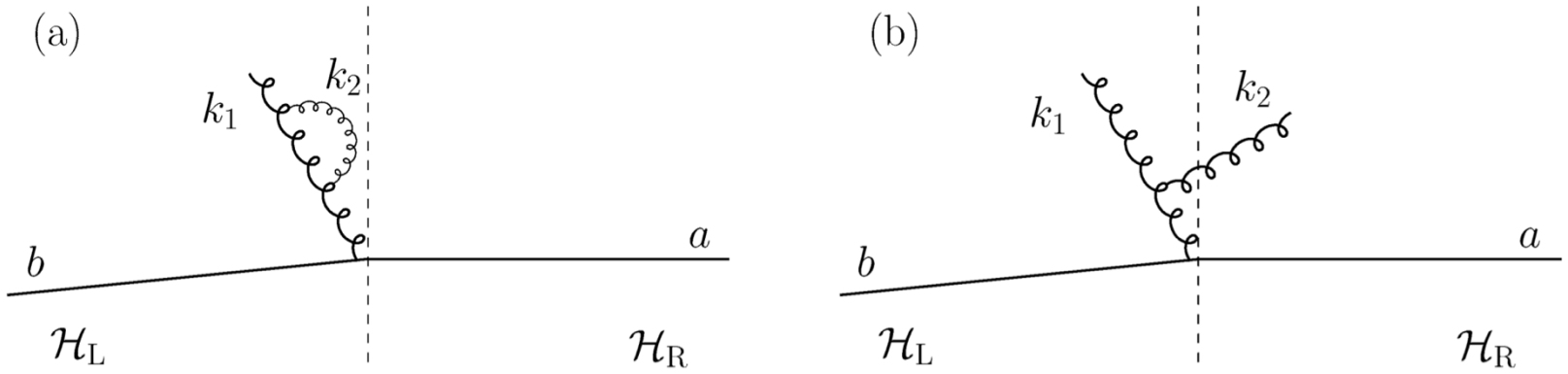

Fig. 1. Kinematic configurations of interest.

$$\frac{1}{2}\mathbf{D}_a^2 = \sum_{i<j}(-\mathbf{T}_i\cdot\mathbf{T}_j)\,\omega_{ij}(\hat{k}_a)$$

$$\mathbf{V}^{\rm in}_{a,b} \approx 1 - \frac{\alpha_s}{\pi}\int_a^b \frac{{\rm d}E}{E}\sum_{i<j}(-\mathbf{T}_i\cdot\mathbf{T}_j)\int_{\rm in}\frac{{\rm d}\Omega}{4\pi}\omega_{ij}$$

$$\Sigma_1(\rho) = \frac{1}{\sigma}\int_0^\rho \frac{{\rm d}\sigma}{{\rm d}\rho}{\rm d}\rho = \frac{1}{N}\int_{\rm out}{\rm d}\Pi_1\ \Big[{\rm Tr}(\mathbf{V}^{\rm in}_{\rho,E_1}\mathbf{D}_1^\mu\mathbf{V}^{\rm in}_{E_1,Q}\mathbf{V}^{\rm in\dagger}_{E_1,Q}\mathbf{D}^\dagger_{1\mu}\mathbf{V}^{\rm in\dagger}_{\rho,E_1})+$$
$${\rm Tr}(\mathbf{V}^{\rm in}_{\rho,E_1}\boldsymbol{\gamma}_1\mathbf{V}^{\rm in}_{E_1,Q}\mathbf{V}^{\rm in\dagger}_{\rho,Q}) + {\rm Tr}(\mathbf{V}^{\rm in}_{\rho,Q}\mathbf{V}^{\rm in\dagger}_{E_1,Q}\boldsymbol{\gamma}_1^\dagger\mathbf{V}^{\rm in\dagger}_{\rho,E_1})\Big]\ .$$

hemisphere jet mass

$$\Sigma_1(\rho) \approx -\frac{NC_F}{2}\zeta(2)\left(\frac{\alpha_s}{\pi}\right)^2\ln^2(Q/\rho)$$

need Σ_n for n > 1 even for leading logs = very complex colour

Trying to understand NGLs = discovery of SLLs

Forshaw, Kyrieleis, Seymour 2006

We now have the machinery to state the all-orders cross-section for one gluon outside of the gap. For the real emission we have

$$\sigma_R = -\frac{2\alpha_s}{\pi}\int_{Q_0}^{Q}\frac{dk_T}{k_T}\int_{\text{out}}\frac{dy\ d\phi}{2\pi}$$
$$\mathbf{M}_0^\dagger \exp\left(-\frac{2\alpha_s}{\pi}\int_{k_T}^{Q}\frac{dk'_T}{k'_T}\mathbf{\Gamma}^\dagger\right)\mathbf{D}_\mu^\dagger \exp\left(-\frac{2\alpha_s}{\pi}\int_{Q_0}^{k_T}\frac{dk'_T}{k'_T}\mathbf{\Lambda}^\dagger\right)\mathbf{S}_R$$
$$\exp\left(-\frac{2\alpha_s}{\pi}\int_{Q_0}^{k_T}\frac{dk'_T}{k'_T}\mathbf{\Lambda}\right)\mathbf{D}^\mu \exp\left(-\frac{2\alpha_s}{\pi}\int_{k_T}^{Q}\frac{dk'_T}{k'_T}\mathbf{\Gamma}\right)\mathbf{M}_0 \qquad (2.22)$$

and for a virtual emission

$$\sigma_V = -\frac{2\alpha_s}{\pi}\int_{Q_0}^{Q}\frac{dk_T}{k_T}\int_{\text{out}}\frac{dy\ d\phi}{2\pi}$$
$$\left[\mathbf{M}_0^\dagger \exp\left(-\frac{2\alpha_s}{\pi}\int_{Q_0}^{Q}\frac{dk'_T}{k'_T}\mathbf{\Gamma}^\dagger\right)\mathbf{S}_V\right.$$
$$\left.\exp\left(-\frac{2\alpha_s}{\pi}\int_{Q_0}^{k_T}\frac{dk'_T}{k'_T}\mathbf{\Gamma}\right)\ \boldsymbol{\gamma}\ \exp\left(-\frac{2\alpha_s}{\pi}\int_{k_T}^{Q}\frac{dk'_T}{k'_T}\mathbf{\Gamma}\right)\mathbf{M}_0 + \text{ c.c.}\right] \qquad (2.23)$$

$$\sigma_{1,\text{SLL}} = -\sigma_0\left(\frac{2\alpha_s}{\pi}\right)^4 \ln^5\left(\frac{Q}{Q_0}\right)\pi^2 Y\ \frac{(3N^2-4)}{480}$$

This is pretty much the result on the previous slide

We expected cancellation in collinear limit

$$\mathbf{\Gamma} = \begin{pmatrix} \frac{N^2-1}{4N}\rho(Y,\Delta y) & \frac{N^2-1}{4N^2}i\pi \\ i\pi & -\frac{1}{N}i\pi + \frac{N}{2}Y + \frac{N^2-1}{4N}\rho(Y,\Delta y) \end{pmatrix}$$

$$\mathbf{\Lambda} = \begin{pmatrix} \frac{N}{4}(Y-i\pi)+\frac{1}{2N}i\pi & \left(\frac{1}{4}-\frac{1}{N^2}\right)i\pi & -\frac{N}{4}s_y Y & 0 \\ i\pi & \frac{N}{4}(2Y-i\pi)-\frac{3}{2N}i\pi & 0 & 0 \\ -\frac{N}{4}s_y Y & 0 & \frac{N}{4}(Y-i\pi)-\frac{1}{2N}i\pi & -\frac{1}{4}i\pi \\ 0 & 0 & -i\pi & \frac{N}{4}(2Y-i\pi)-\frac{1}{2N}i\pi \end{pmatrix}$$
$$+\begin{pmatrix} N&0&0&0\\0&N&0&0\\0&0&N&0\\0&0&0&N \end{pmatrix}\frac{1}{4}\rho(Y,2|y|)+\begin{pmatrix} C_F&0&0&0\\0&C_F&0&0\\0&0&C_F&0\\0&0&0&C_F \end{pmatrix}\frac{1}{2}\rho(Y,\Delta y)$$
$$+\begin{pmatrix} -\frac{N}{4}&0&-\frac{N}{4}s_y&\frac{1}{4}s_y\\0&-\frac{N}{4}&0&\frac{N}{4}s_y\\-\frac{N}{4}s_y&0&-\frac{N}{4}&-\frac{1}{4}\\s_y&\left(\frac{N}{4}-\frac{1}{N}\right)s_y&-1&-\frac{N}{4} \end{pmatrix}\frac{1}{2}\lambda \qquad (2.19)$$

The $i\pi$ terms in the evolution arising from Coulomb gluons generally destroy the cancellation between real and virtual emissions in the case that the out-of-gap gluon is collinear with one of the incoming partons. In more familiar terms, we appear to have discovered that the 'plus prescription' employed in the splitting functions for collinear evolution fails for emissions with transverse momentum above Q_0. It is particularly interesting that the miscancellation occurs only once one includes the imaginary parts in the evolution matrices.

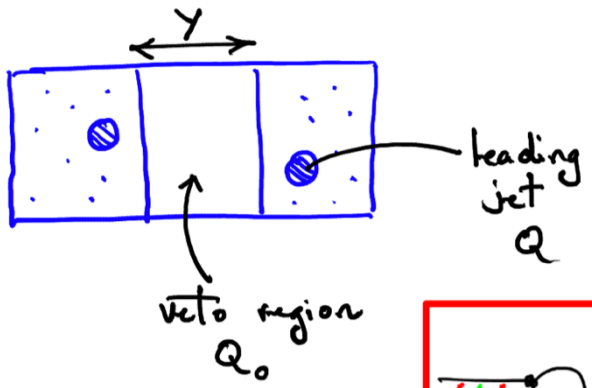

$$\sigma = \sigma_0 + \sigma_1 + \sigma_2 + \cdots$$

$$\sigma_1 = \sigma_1^V - \sigma_1^R$$

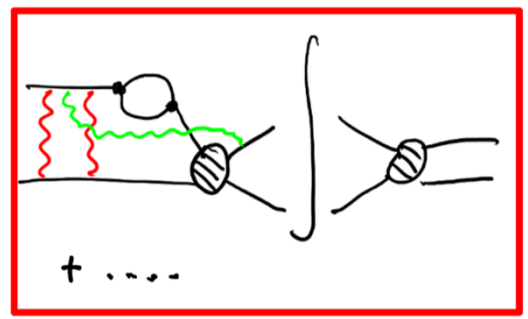

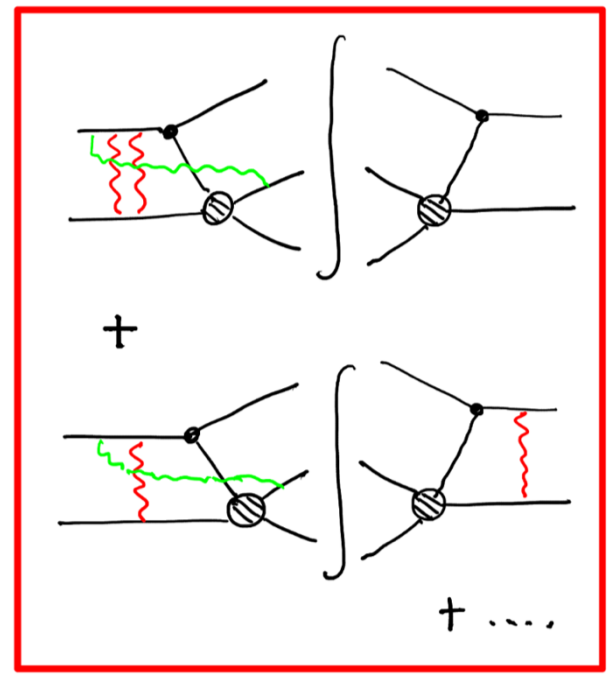

$$\sigma_1 \sim \frac{\alpha_s}{\pi}\int_{Q_0}^{Q}\frac{dk_\perp}{k_\perp}\int^{\ln Q/k_T} dy \times \pi^2 Y\left[\frac{\alpha_s}{\pi}\int_{Q_0}^{k_T}\frac{dk_\perp'}{k_\perp'}\right]^3$$

$$\times\left\{t_1^2\,[[t_4^2,\Delta_c],\Delta_c] - t_1^\dagger\,[[t_4^2,\Delta_c],\Delta_c]\,t_1\right\}$$

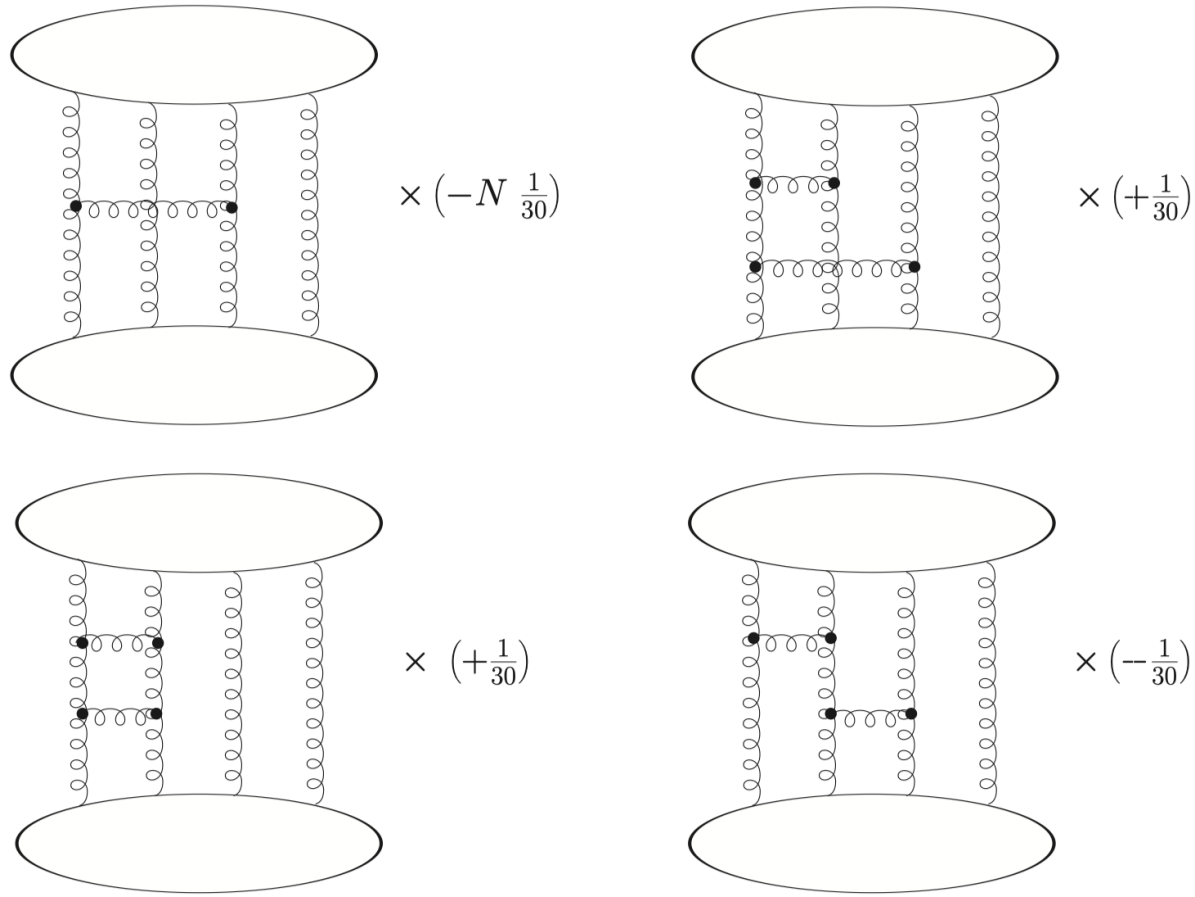

Figure 4: The four diagrams that generate the colour matrix elements when the out-of-gap gluon is the hardest gluon. In the case that the out-of-gap gluon is next-to-hardest, only the first diagram contributes. The upper and lower loops can be quarks, anti-quarks or gluons. Note that these are not Feynman diagrams or even uncut diagrams; they represent only the colour factor of the final result. In the first diagram one of the original six gluon lines has been contracted away, resulting in the additional factor of N.

Resummation

$$\hat{\sigma}^{\mathrm{SLL}}_{2\to M}(Q_0) = \hat{\sigma}_{2\to M}\,\frac{\alpha_s L}{\pi N_c}\left(\frac{N_c\alpha_s}{\pi}\,i\pi L\right)^2 \sum_{n=0}^{\infty} c_n \left(\frac{N_c\alpha_s}{\pi}\,L^2\right)^n$$

Multiple collinear + single soft = simplified colour space

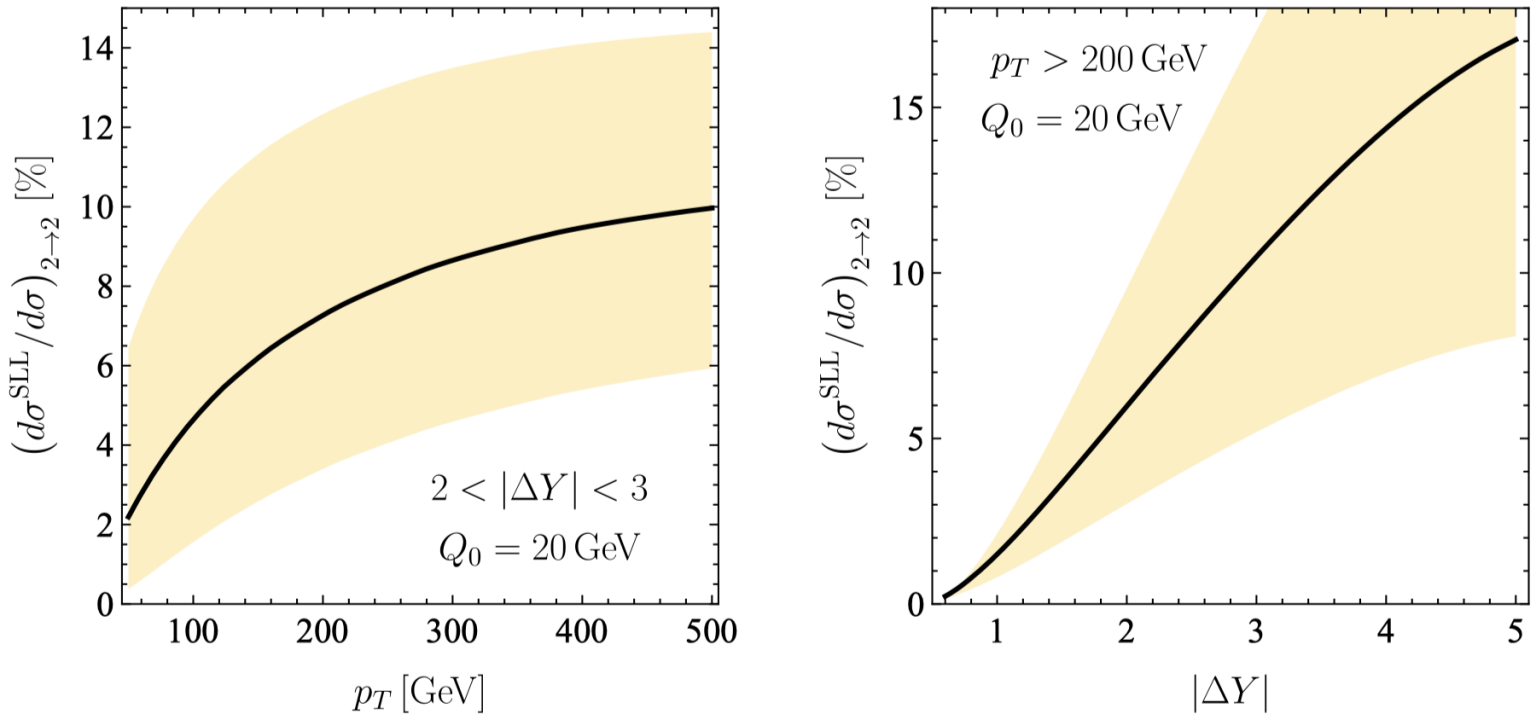

Figure 3. SLL contribution to the differential $pp \to 2\,\mathrm{jets}$ cross section as function of transverse momentum p_T (left) and gap size $|\Delta Y|$ (right). The veto scale is fixed to $Q_0 = 20\,\mathrm{GeV}$.

Becher, Hager, Martinelli, Neubert, Schwienbacher, Stiller (2025)
Becher, Neubert & Ding Yu Shao (2021)

Jettiness contains super-super-leading logarithms

$$\tau_1 = \frac{1}{Q}\sum_k \min\{n_a \cdot p_k,\, n_b \cdot p_k,\, n_J \cdot p_k\} \qquad L = \log 1/\tau_1$$

Banfi, Forshaw, Holguin 2025

2010 Stewart, Tackmann, Waalewijn

$$\sigma(\tau_1) = \int_0^{\tau_1} \frac{\mathrm{d}\sigma}{\mathrm{d}\tau_1'}\mathrm{d}\tau_1' = \sigma \exp\left(-\frac{\alpha_\mathrm{s}}{2\pi}L^2(2C_F + C_A)\right)$$
$$\times \left[g_0(\alpha_\mathrm{s}L) + \alpha_\mathrm{s} g_1(\alpha_\mathrm{s}L) + \alpha_\mathrm{s}^2 g_2(\alpha_\mathrm{s}L) + \cdots\right].$$

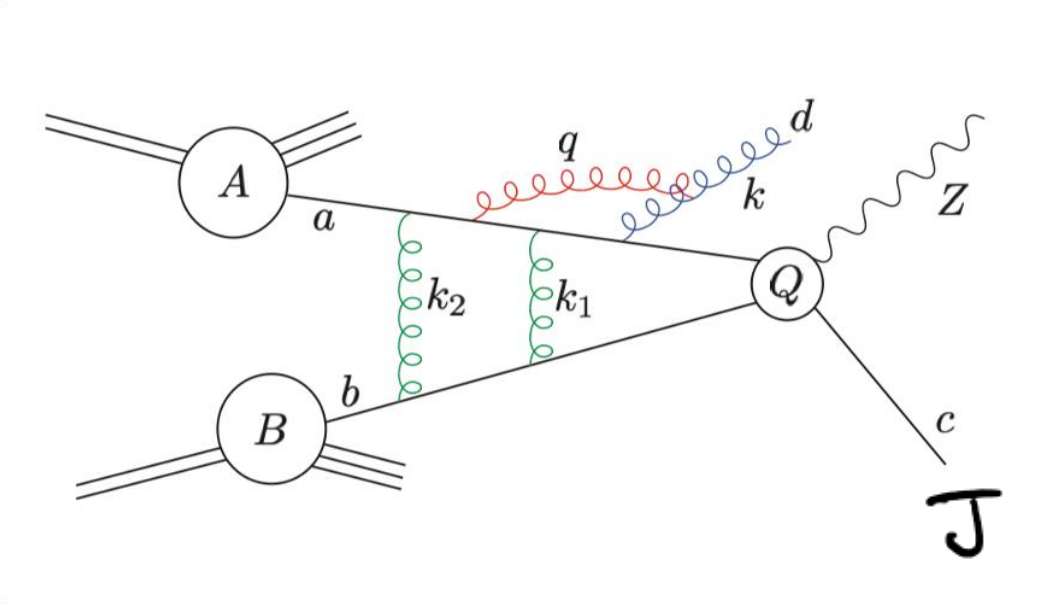

$$\frac{\mathrm{d}\sigma_1^{\mathrm{CVL}}}{\mathrm{d}x_a \mathrm{d}x_b\, \mathrm{d}\mathcal{B}} = \sum_{a=q,g} \frac{\alpha_\mathrm{s}}{\pi} f_A^a(x_a, \mu_\mathrm{F}) f_B^b(x_b, \mu_\mathrm{F})$$
$$\times \int_{\mu_\mathrm{F}}^{Q} \frac{\mathrm{d}k_T}{k_T} \int_{x_a}^{1-\frac{k_T}{Q}} \mathrm{d}z\, \frac{2}{1-z}\, u(k)$$
$$\times\, W_{k_T,Q}\, \mathrm{Tr}(\mathbf{V}^\dagger_{\mu_\mathrm{F},k_T} \mathbf{V}_{\mu_\mathrm{F},k_T} \mathbf{t}_a \mathbf{H}_{ab}(\mathcal{B}) \mathbf{t}_a^\dagger),$$

Extra log is from phase-space volume

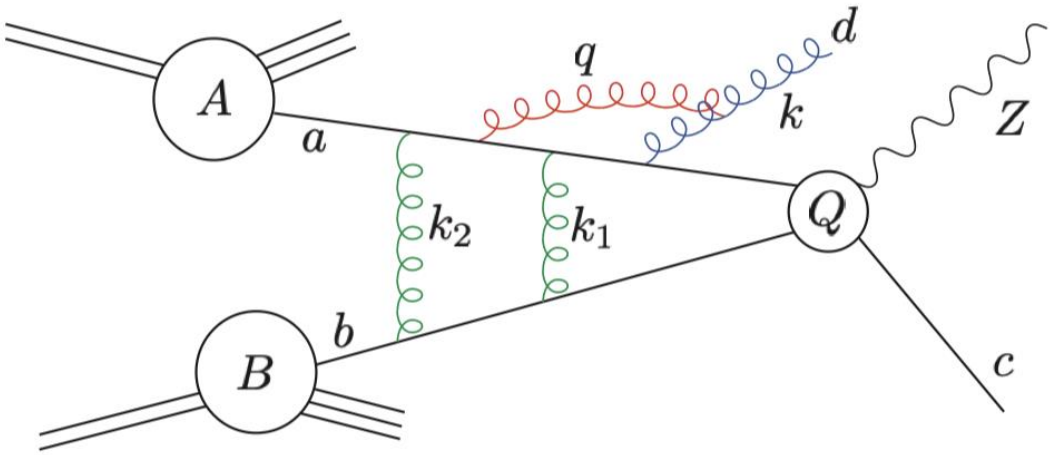

$$\mathbf{V}^{\dagger}_{\mu_F,k_T}\mathbf{V}_{\mu_F,k_T} = \exp\left(\frac{2\alpha_s}{\pi}\mathbf{T}^2_{ad}L_2(\mu_F,k_T)\right. \qquad (13)$$

$$-\left(\frac{\alpha_s}{\pi}\right)^2 L_2(\mu_F,k_T)(-i\pi)\ln\frac{k_T}{\mu_F}[\mathbf{T}^2_{ad},\mathbf{T}^2_s]+$$

$$\left.\left(\frac{\alpha_s}{\pi}\right)^3 L_2(\mu_F,k_T)\left((-i\pi)\ln\frac{k_T}{\mu_F}\right)^2\frac{1}{3}[\mathbf{T}^2_s,[\mathbf{T}^2_s,\mathbf{T}^2_{ad}]+\ldots\right).$$

$$L_2(\mu_F,k_T) = \ln\left(\frac{k_T}{\tau_1 Q}\right)^2 - \ln\left(\frac{\mu_F}{\tau_1 Q}\right)^2$$

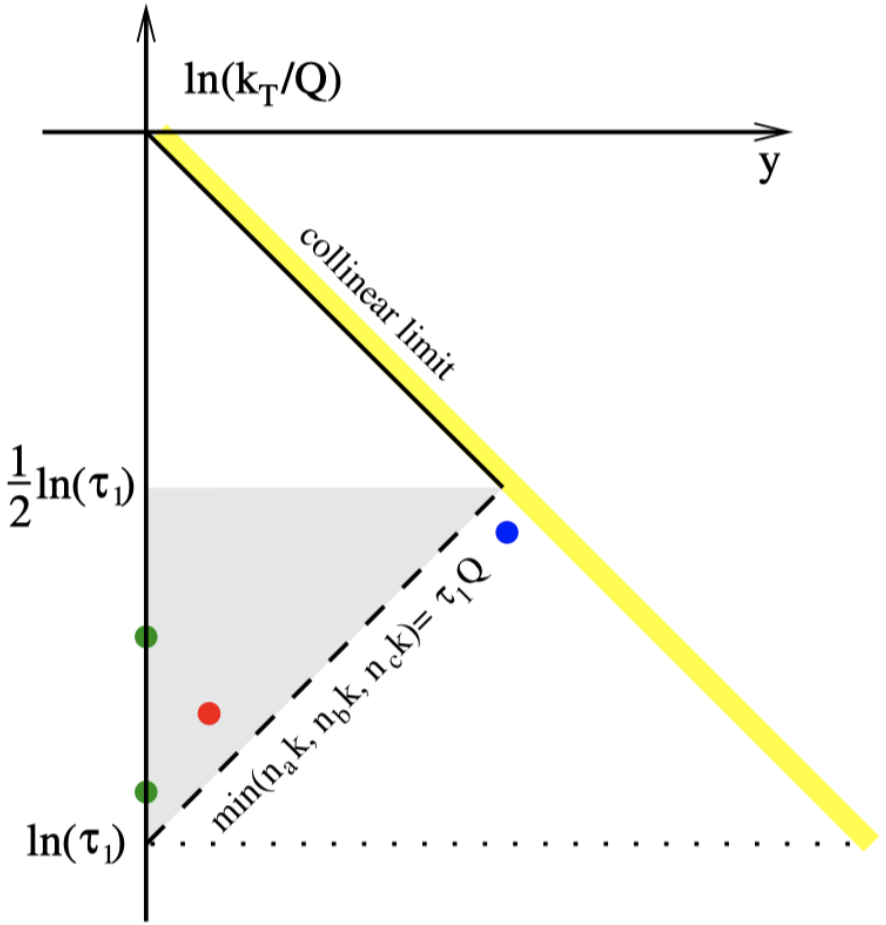

Non-exponentiation of double logs
Resummation more challenging

$$\frac{\mathrm{d}\sigma_1^{\mathrm{CVL}}}{\mathrm{d}x_a\mathrm{d}x_b\mathrm{d}\mathcal{B}} \approx \sum_{a=q,g} A_a\left(\frac{\alpha_s}{\pi}\right)^4(-i\pi)^2\frac{1}{480}\left(\ln\frac{1}{\tau_1}\right)^6$$

Uncharted Logarithmic Structures in QCD Transverse-Energy Flow

Mrinal Dasgupta,[1,*] Alexander Fraley,[1,†] Pier Francesco Monni,[2,‡] and Saad Nabeebaccus[1,§]

[1] *Department of Physics & Astronomy, University of Manchester, Manchester M13 9PL, United Kingdom*
[2] *CERN, Theoretical Physics Department, CH-1211 Geneva 23, Switzerland*

We investigate the QCD transverse-energy (E_T) flow distribution within an azimuthal region of phase space, defined by an angular interval $\Delta\phi$ on the plane transverse to a chosen jet axis. Vetoes on the resulting E_T are widely employed at the LHC to isolate missing transverse momentum in final states with invisible particles. We show that this observable has logarithmic structures never seen before in QCD calculations. Notably, its description involves the resummation of non-global and coherence-violating logarithmic contributions that are more singular than any reported to date. We analyze its all-orders behavior, providing analytical resummations at next-to-double-logarithmic accuracy for e^+e^- and pp collisions, and numerical resummations at leading-logarithmic accuracy in the Veneziano limit for pp collisions. We further present a computation of the leading coherence-violating correction for pp collisions. The intricate structure of vetoes in azimuthal gaps reveals new aspects of QCD dynamics and offers a novel probe of collinear-factorization breaking at the LHC.

$$\Sigma = \frac{1}{\sigma_0}\int_0^{E_T} dE_{T,\Omega}\,\frac{d\sigma}{dE_{T,\Omega}}, \qquad E_{T,\Omega} = \sum_{k_i\in\Omega} k_{t,i},$$

$$\Sigma^{(\mathrm{DL})}_{\mathrm{WTA}} = e^{-4C_F f\bar{\alpha}L^2}.$$

$$\Sigma^{(\mathrm{CVL})}_{\mathrm{DY}} = -\left(\frac{\alpha_s}{\pi}\right)^5 \pi^2 C_F N_c^2 f\,(1-f)^2\,\frac{L^8}{180},$$

$$f = \Delta\phi/2\pi$$

$$\hat{\sigma}_{\mathrm{CVL}} = \left(-\frac{2\alpha_s}{\pi}\right)^5 (1-f)^2 \int_{E_T}^{Q}\frac{dk_{t,3}}{k_{t,3}}\int_{-\eta_3^{\max}}^{\eta_3^{\max}} d\eta_3 \int_{E_T}^{k_{t,3}}\frac{dk_{t,4}}{k_{t,4}}\int_{-\eta_4^{\max}}^{\eta_4^{\max}} d\eta_4 \int_{E_T}^{k_{t,4}}\frac{dk_t}{k_t}$$
$$\left[\frac{1}{3}\ln^2\left(\frac{k_{t,4}}{E_T}\right)\langle m_0|\boldsymbol{D}^{\mu_3\,\dagger}_{a_3,(2)}\boldsymbol{D}^{\mu_4\,\dagger}_{a_4,(3)}\left[\boldsymbol{\Gamma}^{\mathrm{I}}_{(4)},\left[\boldsymbol{\Gamma}^{\mathrm{I}}_{(4)},\boldsymbol{\Gamma}^{\mathrm{R}}_{(4)}\right]\right]\boldsymbol{D}^{\mu_4}_{a_4,(3)}\boldsymbol{D}^{\mu_3}_{a_3,(2)}|m_0\rangle\right] + \mathcal{O}(\alpha_s^6).$$

Becher, Hager, Neubert, Schwienbacher 2026:

"Our findings imply that most existing factorization formulas for global LHC observables must be revised"

Going beyond the leading colour approximation: parton showers at amplitude-level

$$\mathbf{A}_n(E) = \mathbf{V}_{E,E_n}\mathbf{D}_n^{\mu}\mathbf{A}_{n-1}(E_n)\mathbf{D}_{n\mu}^{\dagger}\mathbf{V}_{E,E_n}^{\dagger}\Theta(E \leq E_n),$$

$$d\sigma_n = \mathrm{Tr}\mathbf{A}_n d\Pi_n,$$

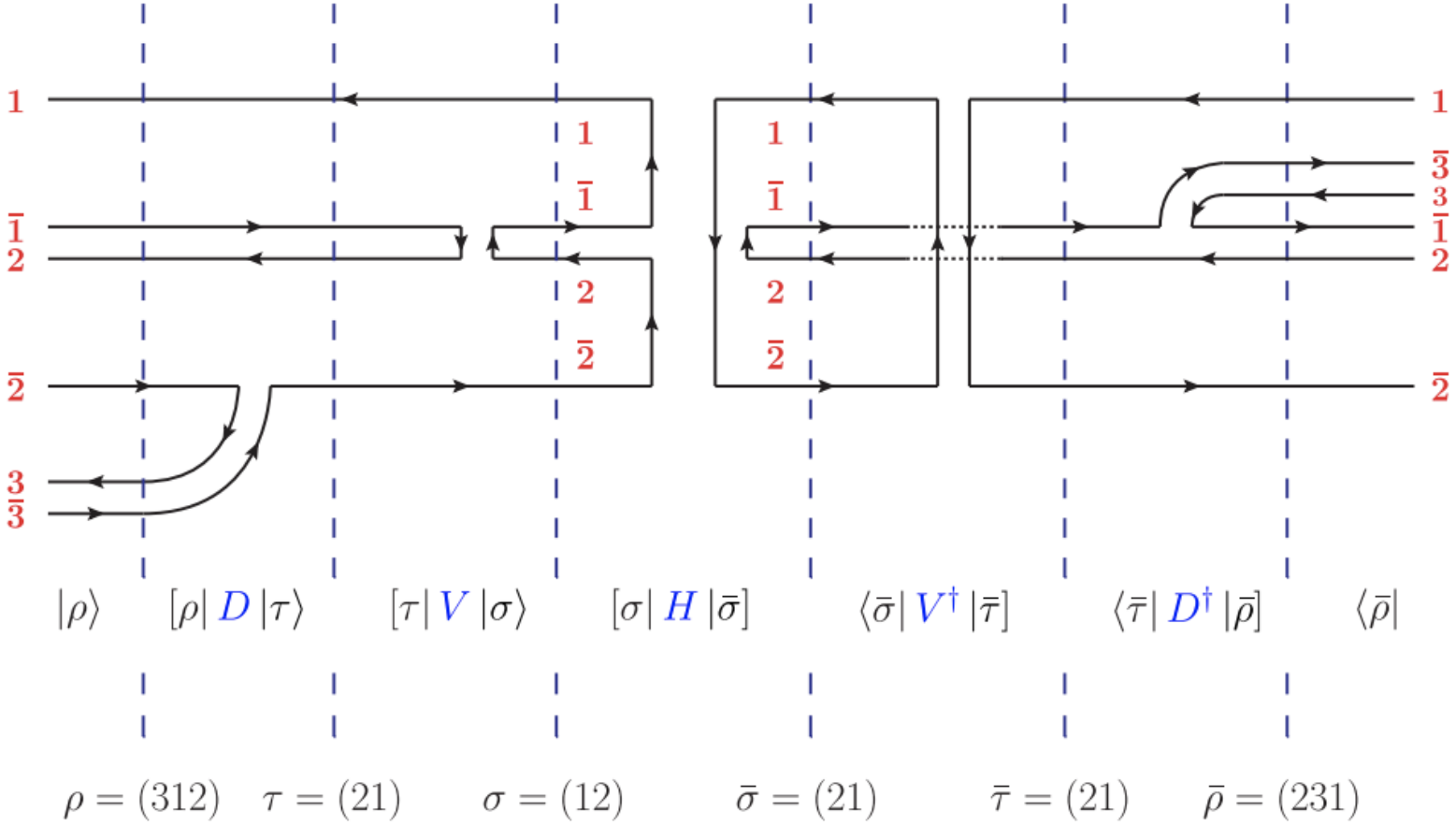

`CVolver`:
2014 Plätzer
2021 de Angeles, Forshaw, Plätzer
2025 Torre González, Forshaw, Plätzer

Nagy & Soper:
2007 "Parton showers with quantum interference"
2012 "Parton shower evolution with subleading color" (LC+)
2014 `DEDUCTOR`
2015 "Effects of subleading color in a parton shower"

CVolver tracks the $1/N_c$ factors as follows:

1. Select an initial pair of flows from the hard scatter matrix. This may be associated with an explicit factor $1/N_c^p$.

2. Emit a gluon in the amplitude and its conjugate. If the gluon is a singlet, it is associated with a factor $1/N_c$, which means any emission is associated with a factor $1/N_c^q$ where $q = 0, 1$ or 2. After the emission, count the minimum number of swaps (r) by which the colour flows in the amplitude and conjugate amplitude differ. If this would be the final emission, there would then be a colour suppression of $1/N_c^r$ from the scalar product matrix, $\underline{\mathbf{S}}$, and the total suppression factor would be $1/N_c^{q+r}$. Crucially, if this is not the final emission it is not possible for further emissions to reduce the degree of colour suppression. This means that the cumulative suppression after the first real emissions is $p + (q + r)$.

3. Operate with the virtual evolution operator in the amplitude and its conjugate. This is done according to the d-expansion, i.e. for $d = 0$ this will involve zero swaps in the colour flows, for $d = 1$ it will involve up to one swap (i.e. one factor of Σ) in each of the amplitude and conjugate (i.e. potentially two swaps in total) etc. Each swap is associated with a factor $1/N_c$ giving a total suppression of $1/N_c^s$. As in the case of the real emissions, there is a further factor $1/N_c^t$ arising from the scalar product matrix (i.e. the swap pushes the colour flows apart so they differ by at least t swaps). Again, subsequent evolution can never reduce the degree of colour suppression and so the cumulative suppression as this phase is $p + (q + r) + (s + t)$.

4. The entire process repeats for subsequent emissions and we veto the event if the cumulative suppression exceeds the required accuracy. This veto on events if the colour wanders too far from the diagonal is vital in ensuring we can handle multiple gluon emissions.

CVolver tracks all powers in N_C and vetos events that are sub-leading

= can compute to specified accuracy in $1/N_C$

$$[\tau|\mathbf{V}|\sigma\rangle \approx \delta_{\tau\sigma} R(\{\sigma\}) + \sum_{l=1}^{d} \left(-\frac{1}{N_c}\right)^l \sum_{\sigma_0,\sigma_1,\ldots,\sigma_l} \delta_{\tau\sigma_0}\delta_{\sigma_l\sigma} \times \prod_{\alpha=0}^{l-1} \Sigma_{\sigma_\alpha\sigma_{\alpha+1}} R(\{\sigma_0,\sigma_1,\ldots,\sigma_l\}).$$

colour flip operator

e.g. d=1

$$[\tau|\mathbf{V}|\sigma\rangle = \delta_{\tau\sigma} e^{-N_c\Gamma'_\sigma} - \frac{1}{N_c}\Sigma_{\tau\sigma}\frac{e^{-N_c\Gamma'_\tau} - e^{-N_c\Gamma'_\sigma}}{\Gamma'_\tau - \Gamma'_\sigma}$$

Plätzer 2014

Results from `CVolver`

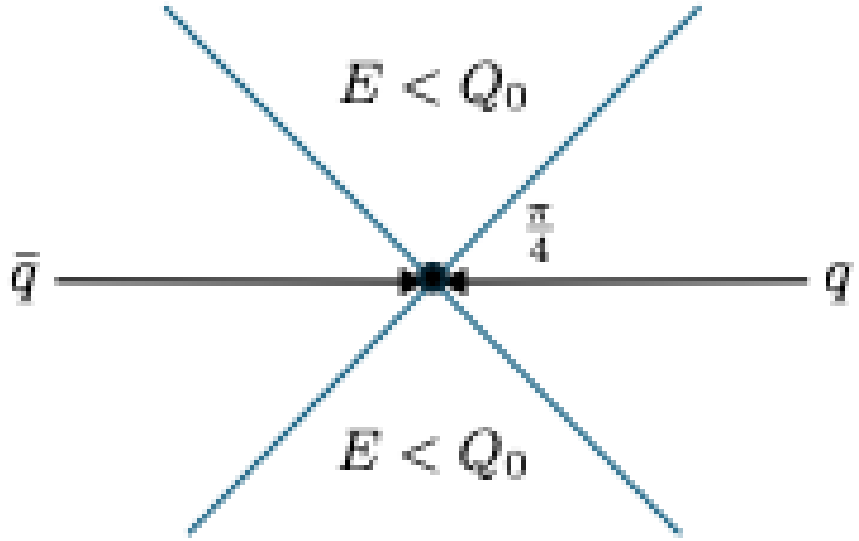

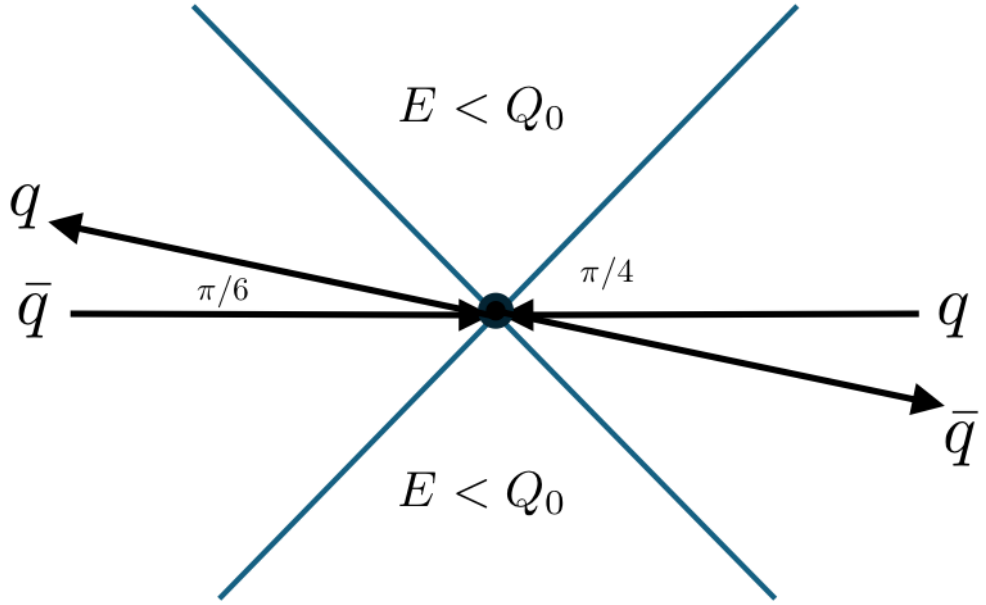

$$\varsigma = Q_0/Q$$

$$H = |10\rangle\langle 10| - \frac{1}{N_c}|10\rangle\langle 01| - \frac{1}{N_c}|01\rangle\langle 10| + \frac{1}{N_c^2}|01\rangle\langle 01|,$$

LCH

nb

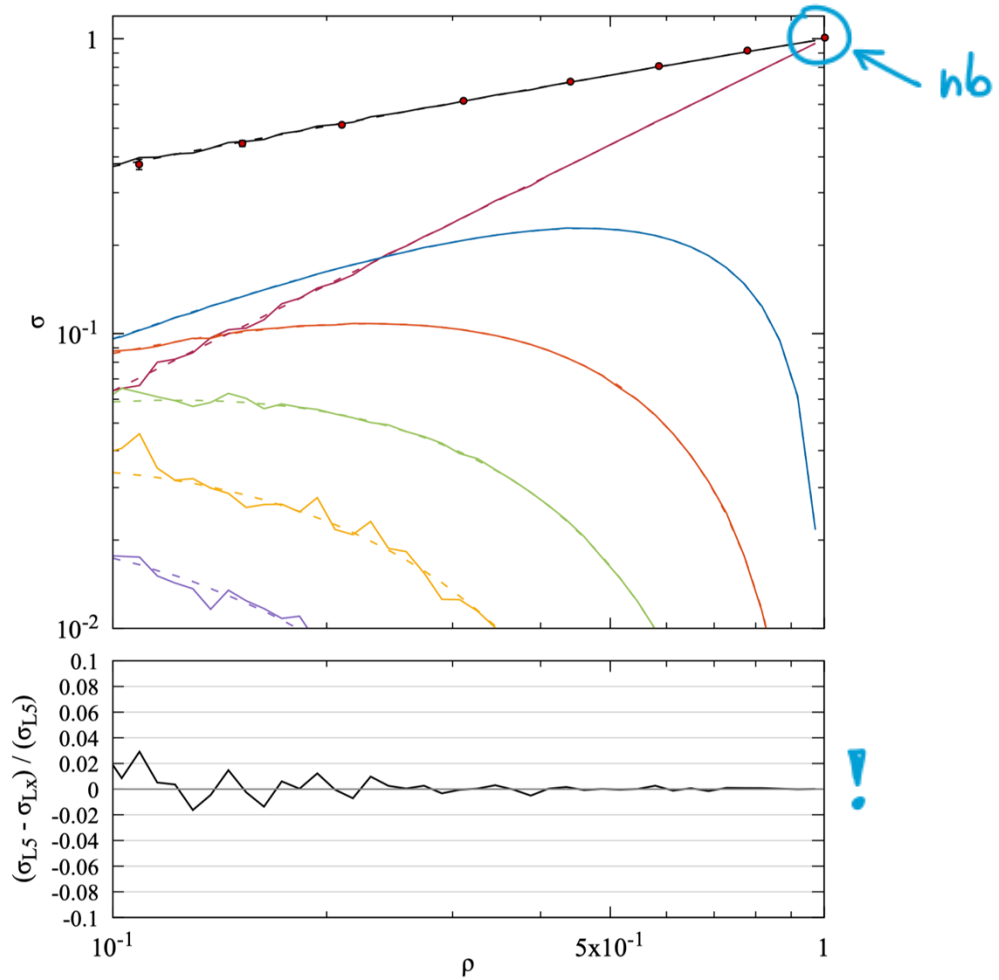

!

Figure 6: The veto cross-section as a function of veto scale for $H \to gg$. Solid: Full colour, Dashed: leading colour. The different coloured curves correspond to different multiplicities (0 up to 5 emissions) and the black curves are the total cross-section. The lower residual plot is for the total cross-section. The red circles are from [17].

See also Hatta & Ueda

Full colour = strict leading colour

$H \to gg$

"Somewhat miraculous given the complexity of the calculation"

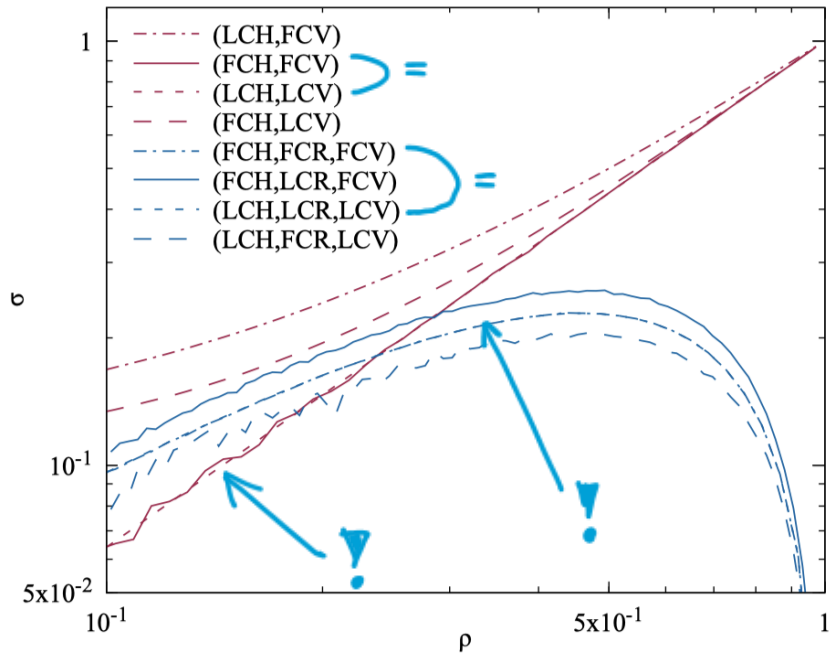

Figure 7: The veto cross-section as a function of veto scale for $H \to gg$. The red curves correspond to 0 emissions, and the blue curves to 1 emission.

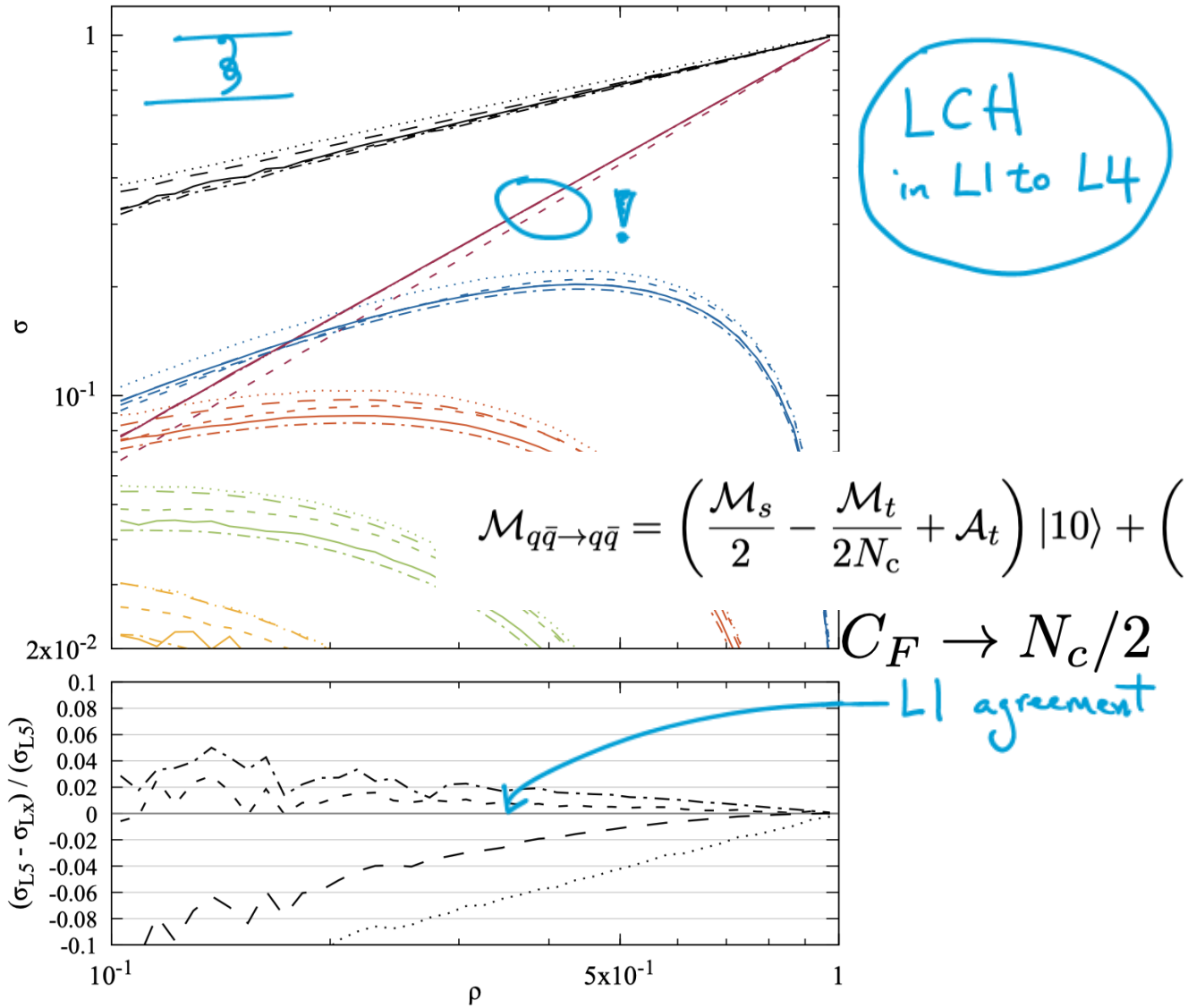

LCH in L1 to L4

$$\mathcal{M}_{q\bar{q}\to q\bar{q}} = \left(\frac{\mathcal{M}_s}{2} - \frac{\mathcal{M}_t}{2N_c} + \mathcal{A}_t\right)|10\rangle + \left(\frac{\mathcal{M}_t}{2} - \frac{\mathcal{M}_s}{2N_c} + \mathcal{A}_s\right)|01\rangle.$$

$C_F \to N_c/2$

L1 agreement

ure 17: The veto cross-section for the t-channel gluon exchange contribution to $q\bar{q} \to$ Solid: Full colour (L5), Dash-dotted: LC′ + FCR (L4), Long-dashed: LC′ + LCR inglets (L3), Dotted: LC′ + LCR (L2), Short-dashed: strict LC (L1). For the L1–L4 ves we start the evolution using the leading-colour approximation to the hard-scatter rix.

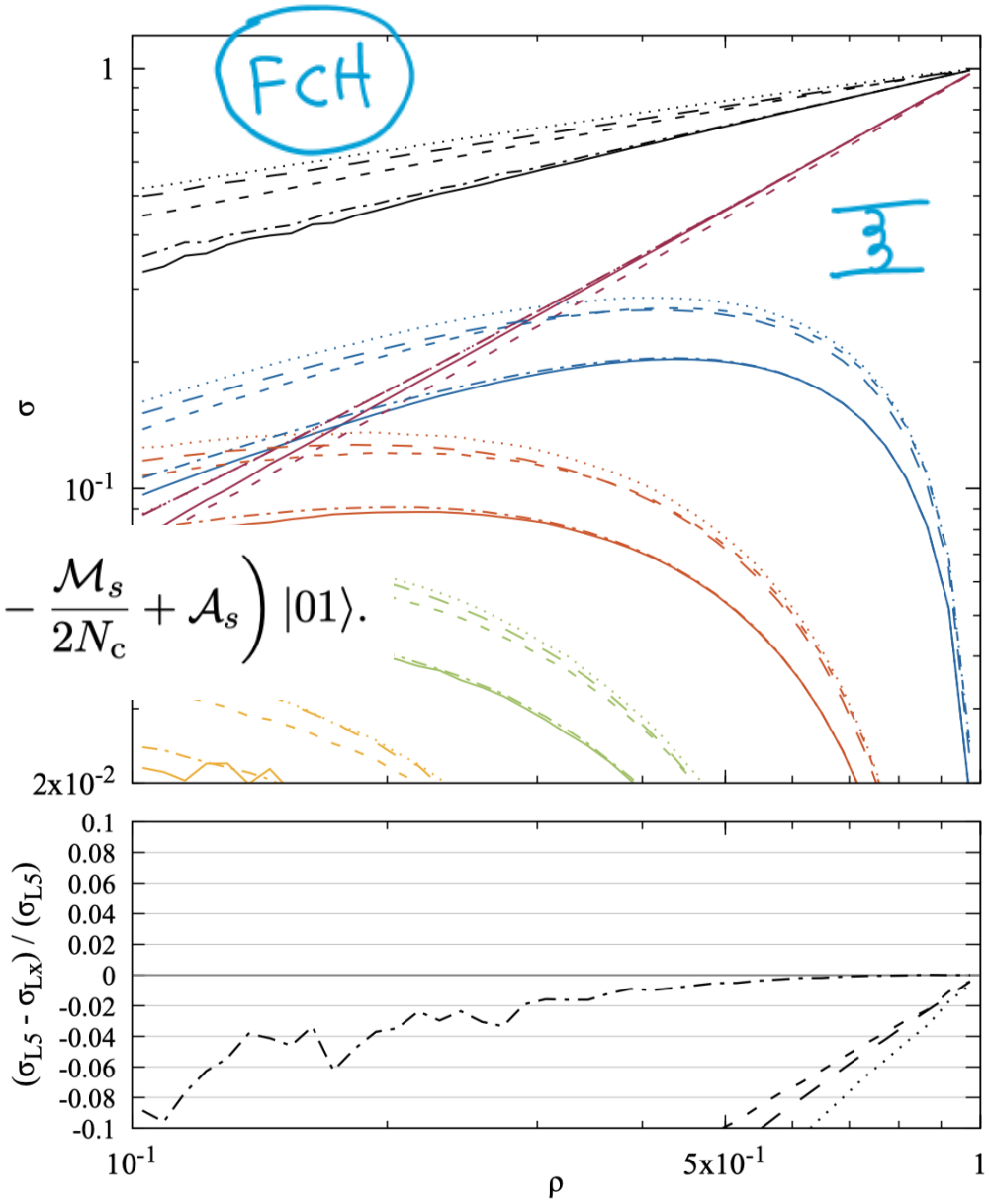

Figure 16: The veto cross-section for the t-channel gluon exchange contribution to $q\bar{q} \to q\bar{q}$. Solid: Full colour (L5), Dash-dotted: LC′ + FCR (L4), Long-dashed: LC′ + LCR + singlets (L3), Dotted: LC′ + LCR (L2), Short-dashed: strict LC (L1).

$$= |3201\rangle + |2310\rangle - |1302\rangle - |2031\rangle$$

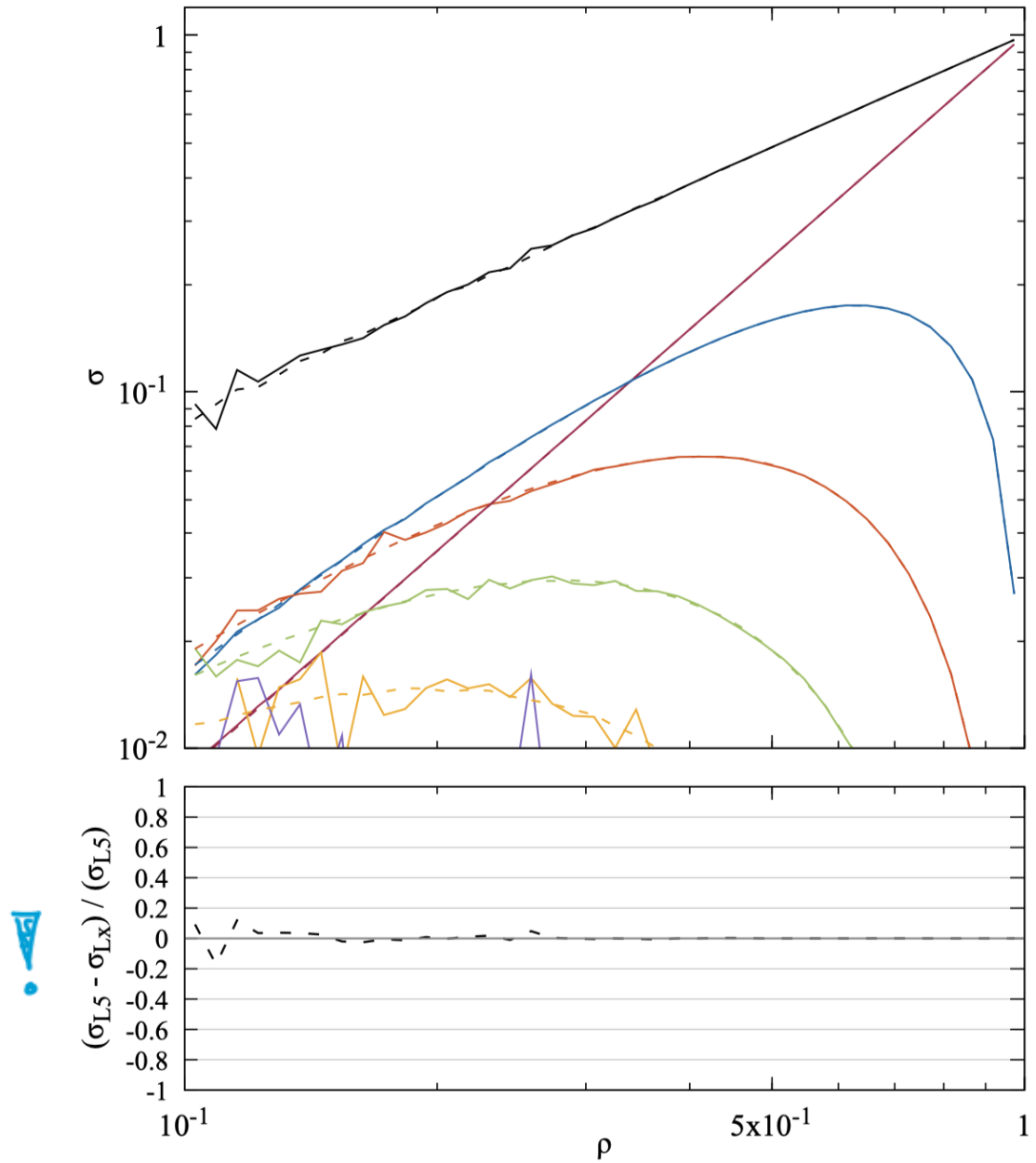

Figure 49: The veto cross-section for the t-channel contribution to $gg \to gg$. Solid: Full colour, Short-dashed: Leading colour.

$$= |3201\rangle + |2310\rangle - |3012\rangle - |1230\rangle$$

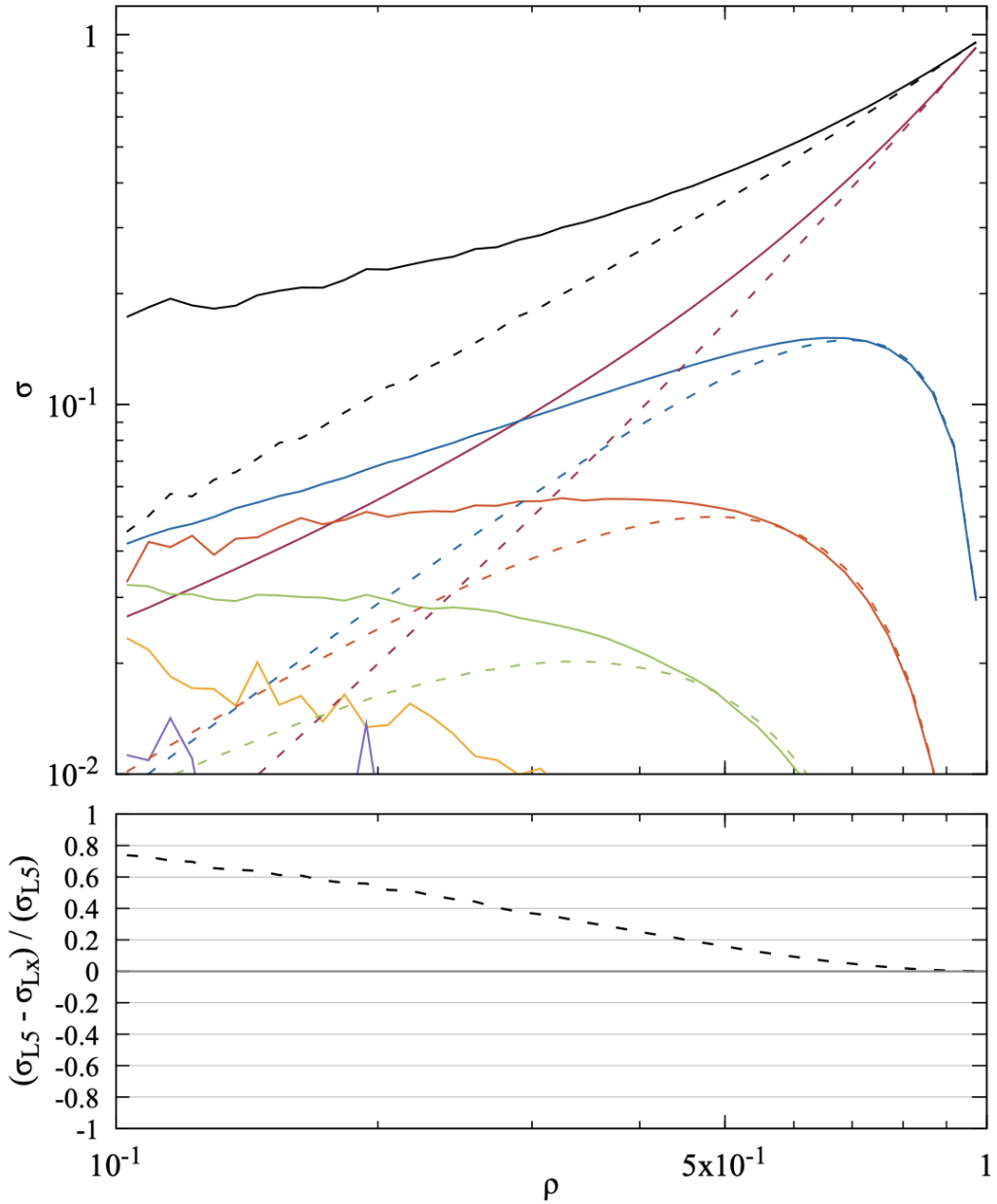

Figure 50: The veto cross-section for the u-channel contribution to $gg \to gg$. Solid: Full colour, Short-dashed: Leading colour.

$$= |3012\rangle + |1230\rangle - |1302\rangle - |2031\rangle$$

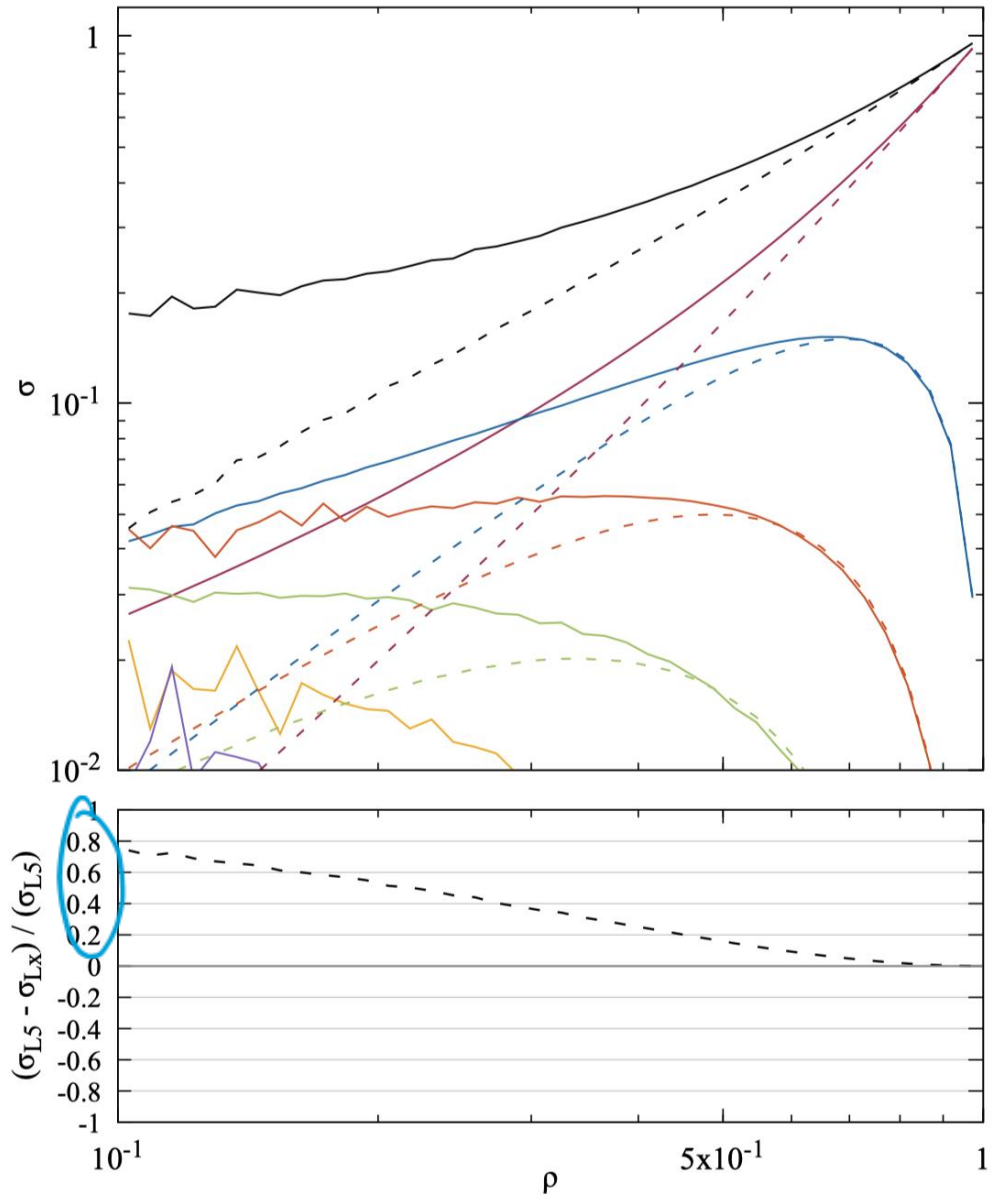

Figure 48: The veto cross-section for the s-channel contribution to $gg \to gg$. Solid: Full colour, Short-dashed: Leading colour.

`CVolver` as a partonic event generator

$$\frac{\mathrm{d}^3\sigma}{\mathrm{d}\Omega\mathrm{d}\rho} = \sum_n \int \mathrm{d}\sigma_n \, \delta\left(\rho - E_i\right) \delta\left(\Omega - \Omega_i\right)$$

i = highest energy soft-gluon in the veto region

$$\frac{\mathrm{d}^2\Sigma(r)}{\mathrm{d}\Omega} = \int_0^r \mathrm{d}\rho \frac{\mathrm{d}^3\sigma}{\mathrm{d}\Omega\mathrm{d}\rho}$$

$$\frac{\mathrm{d}\Sigma(r)}{\mathrm{d}\cos\theta} = \int_0^{2\pi}\int_0^r \mathrm{d}\rho \, \mathrm{d}\phi \frac{\mathrm{d}^3\sigma}{\mathrm{d}\Omega\mathrm{d}\rho}$$

$$\frac{\mathrm{d}\Sigma(r)}{\mathrm{d}\phi} = \int_{-1}^1\int_0^r \mathrm{d}\rho \, \mathrm{d}(\cos\theta) \frac{\mathrm{d}^3\sigma}{\mathrm{d}\Omega\mathrm{d}\rho} \, .$$

$$\int_{\text{veto region}} \frac{d^2\Sigma}{d\Omega} \, d\Omega = \sigma(r)$$

↖ veto cross section

recoil jets

red

green

leading s-channel

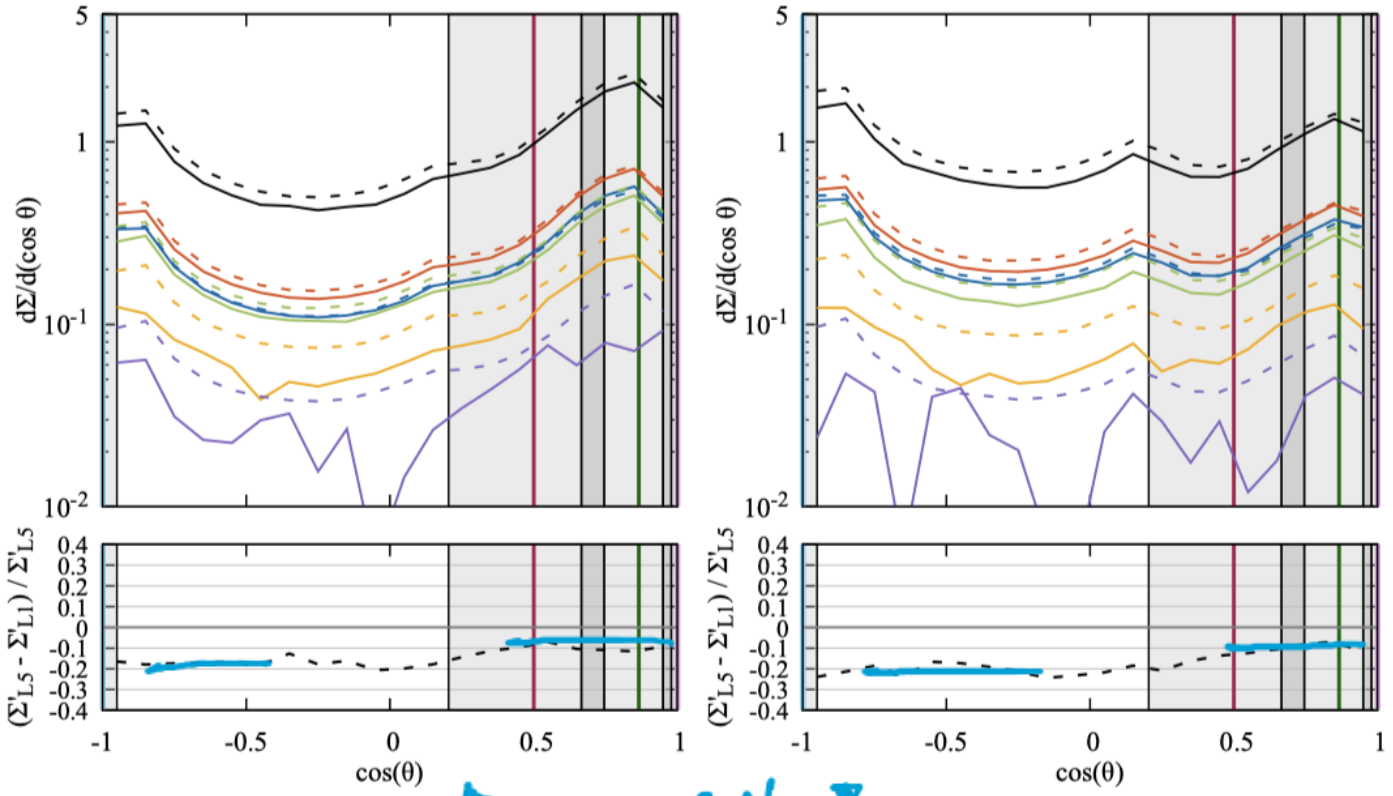

LC fails!

(a) The t-channel gluon exchange contribution. (b) The s-channel gluon exchange contribution.

leading t-channel

Figure 11: The differential cross section $d\Sigma/d(\cos\theta)$ of the different contributions to the $q\bar{q} \to q\bar{q}$ process, in the jets with a recoil configuration, and broken down by multiplicity. The solid curves are obtained using full colour evolution, and the dashed curves use strictly leading colour evolution. For the leading colour curves, we start the evolution using the leading-colour approximation to the hard-scatter density matrix. The locations of the hard jets are marked with vertical lines matching the colours used in Fig. 4. The shaded vertical bars indicate the jet regions. Darker shades indicate an overlap of multiple jet-cones.

Conclusions

Empty rapidity gaps are difficult to calculate. Gap survival, the underlying event and the nature of the pomeron remain unsolved, hard problems notwithstanding a huge amount of experimental and theoretical progress.

The easier problem of wide-angle, soft-gluon resummation remains a major challenge….

Super-leading logarithms phenomenology:

Need full resummation including (S)SLL and non-global logarithms matched to fixed-order to compare to data.

`CVolver`:

Sub-leading colour can easily be >10% in gaps between jets and in some cases much more than that.

Something interesting is happening in the case of t-channel gluon exchange.

For the future: include incoming hadrons, k_T ordering, hard-collinear physics. Early goal: numerical study of CVLs.

Beyond leading log & hadronization: Plätzer 2023